

Silver nanoparticles mediated by extract of Guar plant (*Cyamopsis tetragonoloba*), and evaluation of their photocatalytic and antibacterial properties

Elias E. Elemike^{1,2,3}, Saiyed Tanzim^{1,2}, Anthony C. Ekennia⁴, Damian C. Onwudiwe^{1,2*}

¹Material Science Innovation and Modelling (MaSIM) Research Focus Area, Faculty of Natural and Agricultural Sciences, North-West University, Mafikeng Campus, Private Bag X2046, Mmabatho 2735, South Africa

²Department of Chemistry, School of Physical and Chemical Sciences, Faculty of Natural and Agricultural Sciences, North-West University, Mafikeng Campus, Private Bag X2046, Mmabatho 2735, South Africa

³Department of Chemistry, College of Science, Federal University of Petroleum Resources, P.M.B 1221, Effurun, Delta State, Nigeria

⁴Department of Chemistry, Alex Ekwueme Federal University Ndufu-Alike, PMB 1010, Abakaliki, Ebonyi State, Nigeria

*Corresponding author: Tel: (+27) 18 389 2545; Fax: (+27) 18 389-2420; E-mail: Damian.Onwudiwe@nwu.ac.za

DOI: 10.5185/amlett.2019.2198

www.vbripress.com/aml

Abstract

The green synthesis of silver nanoparticles using *Cyamopsis tetragonoloba* plant extract, and their photocatalytic and antibacterial properties is reported. Three precursor concentrations of 1 mM, 2 mM and 5 mM were used, and at two different ratios of 1:5 and 1:10 plant extract to the precursor. The formation of the nanoparticles was followed by the periodic study of surface plasmon resonance using the UV-visible spectroscopy, which revealed the formation of nanoparticles with regular bands after 45 min. of reaction. Fourier transform infrared spectroscopy was used to study the functional groups present in the plant biomolecules which aided the reduction and stabilization of the nanoparticles. Transmission electron microscopy analysis and X-ray diffraction pattern showed the particle sizes and crystalline structures, while the zeta potential values indicated the stability of the nanoparticles. The 5 mM concentration gave the largest particle sizes of about 12.90 nm and the most stable particles. The photocatalytic properties of the particles studied using Methyl red showed a low efficiency of 17.85% degradation achieved under 2 h. The antibacterial potency of the nanoparticles was screened against some Gram-negative and Gram-positive bacteria. The results showed that the nanoparticles have good antibacterial activities. Copyright © 2019 VBRI Press.

Keywords: Silver nanoparticles, green synthesis, photocatalysis, antibacterial.

Introduction

The diverse properties of nanoparticles and their applications continue to generate more interest, leading to exploring different synthesis route. Different metal nanoparticles have been reported, and interest continue to rise on the behaviour of several noble metal nanoparticles synthesized from many substrates that act as reducing, stabilizing and capping agents. Nanoparticles have interesting properties which are different from their bulk materials such as optical, electrical, thermal and catalytic properties [1, 2]. These properties also differ among the same type of nanoparticles depending on the method of preparation. Silver nanoparticles are interesting noble metal nanoparticles with wide range of applications including consumer products, cosmetics, medical, food, health care and industrial purposes [3-6]. The applications have necessitated for non-toxic methods of synthesis since the nanoparticles synthesized via the conventional methods using chemicals, as capping agents, could gradually release the agents into the consumer and health care products. Other methods of synthesis such

as physical method could involve the use of furnace or spark discharge. Although the synthesis is characterized by short reaction time, the expensive nature, high energy reaction, low yield and non-uniform particle sizes have hindered the wider exploitation of this method [7].

Biological method of nanoparticle synthesis involving the use of molecules such as proteins, sugars, vitamins, amino acids and various secondary metabolites (that have reducing, stabilizing and capping abilities towards the metal ions) have offered greater advantage than the chemical route [8, 9]. One of such secondary metabolites is the active polyphenols which are good natural antioxidants with great potency in nutraceuticals, drugs formulation and food additives [10]. This phytocomponent, along with other components, play important role in the reduction of metal ions and enhancing their biological activities in the synthesized nanoparticles. They are eco-friendly, cheap and aid the production of particles of similar sizes and shapes [11]. The biological synthesis of nanoparticles could either be the micro-organisms mediated method or the phyto mediated synthesis. The

later method involves the use of plant, and this method has attracted lots of interest due to their clean, simple and cost effectiveness. Almost all parts of a plant ranging from the bark, fruits, peels, pods, sap, petals leaves, roots, shoots can be utilised in the synthesis, and they are prepared either fresh or dried to act as the bioreductant [12, 13]. The natural biosurfactant molecules (saponins) in the plant aids in dispersion during the reaction and they are biocompatible, nontoxic and nonionic, which makes them the best alternative to synthetic surfactants and safe to the environment [14]. Other biomolecules present in the plant parts also offer capping and stabilizing ability by their interaction with the particle surface making it unnecessary for additional reagents to perform such functions [15]. The differences in the proportion of these biomolecules among most plants highlight the need for continuing investigation of different plants towards nanoparticle synthesis. For example, Neem plant contains high concentration of terpenoids and flavonoids [16, 17] which aids in the stability and capping effect when used in nanoparticle synthesis; whereas Reetha (*Sapindus mukorossi*) and Shikakai (*Acacia concinna*) have more saponins (biosurfactant) which would cause more reducing property thereby leading to smaller nanoparticles [14]. Other plants could contain higher quantities of some other metabolites thereby placing them at a particular advantage over others.

During the biosynthesis reaction, the reaction temperature, nature and concentration of substrate, and precursor concentration play crucial role in controlling the morphology, particle size and surface chemistry of the nanoparticles [18, 19]. As a result of this, there are continued efforts to explore different synthesis route in order to obtain smaller sizes of nanoparticles because they have shown to possess more improved properties [11].

Nanosilver has wide applications especially in nanomedicine [20, 21]. They have been used in theranostics such as photothermal therapy to locate and destroy cancer cells, and as biosensor for detection of squamous cell carcinoma [22, 23]. Multifunctional silver-embedded magnetic nanoparticles have been used to locate breast cancer cells and leukemia [24], which reiterates the toxic potential of plant-based silver nanoparticles against carcinoma cells [8]. In recent times, infections in open wounds and chronic ulcers have been treated using nanosilver based dressings [25]. Other biological and medical applications include as antimicrobial [26, 27], anti-inflammatory, anti-viral, anti-angiogenesis and anti-platelet [28, 29] larvicidal agents [30]. Silver has also found applications in other areas; Etherigde *et al.* [31] reported the hybrid of silver nanoparticles with vanadium oxide which could enhance the battery performance in the next-generation active implantable medical devices. Another interesting field where AgNPs have found diverse use is in redox catalysis and photocatalysts where they promote electron transfer and give access to the low activation

energy reaction [32]. As photocatalysts, they enhance the photo-degradation of organic pollutants in water thereby serving efficiently in water purification and environmental remediation [33, 34]. Other reports on plant mediated biosynthesis of silver nanoparticles include *Nigella arvensis* [35], *Phyllanthus amarus* [36], banana peels [37], *Ocimum sanctum* [38], *Laminaria japonica* [39], Andean blackberry fruit extract [40] etc.

In this research, we have synthesized silver nanoparticles using Guar bean leaf. Guar is a plant which originates from Africa, but it has been cultivated throughout Asia especially in India. This plant, which is also known as Cluster bean plant, has been much appreciated for its gum obtained from the endosperm of the seeds which has many applications in paper, food, mining, cosmetics, textile, oil and pharmaceutical industries [41]. Its flavonoid contains quercetin, daidzein, kaemferol, and 3-arabinsides [42]. Cluster bean (*Cyamopsis tetragonoloba*) is a rich source of soluble fibre and is recognized for its cholesterol reducing effect [43]. Guar gum – a galactomannan has been shown to be a potent hypocholesterolaemic agent in both normal and hypercholesterolaemic animals [44]. These cluster or guar beans are also helpful in building bones, teeth, maintaining blood pressure and resolving anaemia. The beans have antidiabetic effect, antiulcer, cytoprotective and anticholinergic effect, hypoglycemic and hypolipidemic effect, antiasthmatic and anti-inflammatory activities on human body [45]. Here, the leaf extract of the plant was used with different concentrations of the precursor compound (AgNO_3) in order to study the effect of the change in concentration on nanoparticle size and determine the antibacterial and photocatalytic properties of the as-synthesized silver nanoparticles.

Materials and methods

Preparation of aqueous Guar leaf extract

The Guar plant was sourced from Mafikeng, South Africa and properly identified by a botanist at North West University. The leaves were washed to remove the dirt and soil debris. It was, thereafter, dried and blended into powder. The powdered leaf was boiled at about 80 °C using double-distilled water for an hour and filtered. The filtrate now served as the reaction substrate and was used for the synthesis of AgNPs.

Synthesis of Guar leaf mediated silver nanoparticles (GAgNPs)

Silver nanoparticles were biosynthesized using the reported literature method with little modification [46, 47]. Aqueous solutions of the metal salts (1 mM, 2 mM and 5 mM) silver nitrate were prepared using double distilled water and added to the aqueous leaf extract. In each of the precursor concentration, the obtained nanoparticles were synthesized using the ratio of (1:5 and 1:10) leaf extracts to the metal ion solutions. The reaction mixture was stirred at the temperature of about 80 °C for two hours with periodic sampling of the

nanoparticle solution to study the formation of silver nanoparticles.

Characterisation of the silver nanoparticles

UV-visible spectrophotometer was used to monitor the stages in the formation of the silver nanoparticles as aliquots were taken at regular time intervals. The particle sizes of the synthesized AgNPs were estimated using JEOL2100 Transmission electron microscopy (TEM) instrument (München, Germany) fitted with a LaB 6 electron gun at 5 kV, and images were captured using Ultrascan digital camera. The particle size distribution was obtained using Image J software. The samples were prepared by firstly sonicating for an hour, after which drops of the sample were placed on the TEM copper grids, followed by drying and evaporation. The functional groups present in the biocomponents involved in reducing, stabilizing and capping of the AgNPs were verified by the aid of Bruker alpha-P FT-IR spectrophotometer in the wavenumber range $400 - 4000 \text{ cm}^{-1}$. The surface charges and zeta potential values were determined using the laser zeta meter (Malvern zetazizer 2000, Malvern). The samples were dissolved in about 50 mL double distilled water, sonicated and filtered. The zeta potential was then measured at solution pH of 7.

Photocatalytic studies of the GAgNPs

The behaviour of the GAgNPs as photocatalysts in the degradation of methyl red was studied under UV irradiation. An aqueous solution of 20 mg/L of the methyl red was prepared and properly stirred. Afterwards, 100 mL was taken from the original stock solution of methyl red and 20 mg of GAgNPs was introduced into it. They were properly stirred in the dark for equilibration before being subjected to the UV irradiation. The solution was constantly stirred and aliquot of the samples were taken at intervals using UV-vis spectrophotometer to determine the extent of degradation of the methyl red.

Antibacterial analysis of the as-synthesized GAgNPs

The GAgNPs were analysed for their antibacterial activity using the agar well diffusion method with slight modification from reported methods. The bacterial strains used were Gram-negative *Escherichia coli*, *Klebsiella pneumonia* and Gram-positive *Staphylococcus aureus* and *Bacillus cereus*. The organisms were seeded in agar plates using sterile Muller-Hinton agar (MHA, Sigma-Aldrich USA, 97.5%) by the "pour plate" technique. Five holes were made using a cork borer and GAgNPs solutions (0.05, 0.1, 0.25, 0.5 mg/mL) were introduced. Ciprofloxacin, used as positive control, was introduced into one of the holes. They were all incubated for 24 h at 37°C and approx. $10 \mu\text{L}$ of 1.25 mg/mL 3-(4, 5-dimethylthiazol-2-yl)-2, 5-diphenyltetrazolium bromide (MTT) was introduced into the samples to afford a purple colouration, indicating microbial growth. The formation of a clear zone around the hole is an indication of antibacterial activity, but values $<6 \text{ mm}$ do not portray

antibacterial potentials. The experiments were repeated twice in order to get replicate results of zones of inhibition recorded in millimetres. The experimental results were given as mean \pm S.D. of the two parallel measurements.

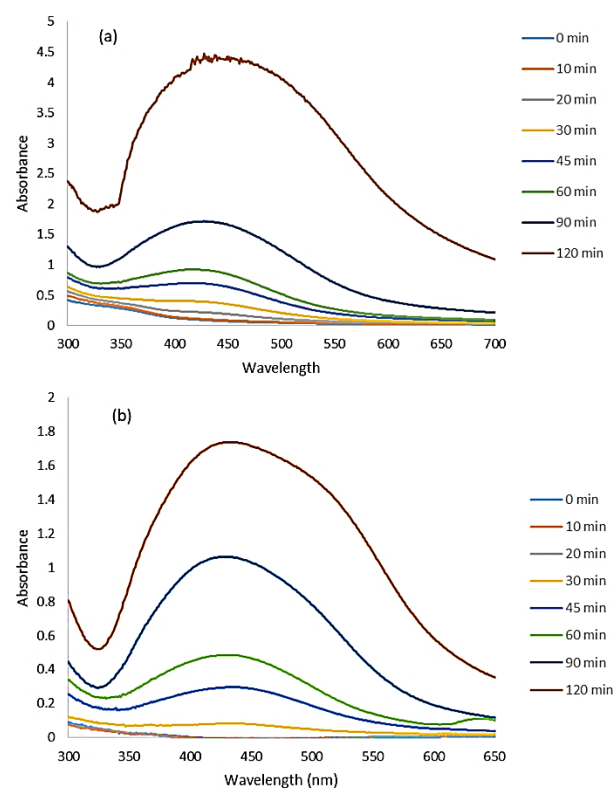


Fig. 1. UV-visible spectra of the Ag nanoparticles synthesized using 1 mM AgNO_3 at (a) 1:5 and (b) 1:10 substrate to precursor.

Results and discussions

UV-visible spectroscopy analysis of the GAgNPs

Figs. 1-3 show the absorption spectra of the GAgNPs obtained at different concentrations. In all the spectra, evidence of formation of AgNPs was noticed after 45 min of the reaction. All the peaks were broad indicating polydispersity of the AgNPs, except in the particles prepared from 2 mM AgNO_3 using 1:10 ratio. In all the formulations, the GAgNPs from 1 mM AgNO_3 using 1:5 ratio has the highest concentration of nanoparticles at 434 nm. Similar absorption peak was observed in the GAgNPs prepared from 1:10 ratio. In the particles prepared from 2 mM AgNO_3 using 1:5, a higher peak (449 nm) was obtained compared to the spectrum obtained using 1:10 ratio (which has peak of absorption around 440 nm). The lower absorption peak of the samples from 1:10 ratio suggests smaller particle size [48]. In the GAgNPs from 5 mM concentration, the 1:5 ratio has lower absorption peak of 447 nm compared to the 449 nm exhibited by the 1:10 ratio. This shows that the lower the wavelength, the smaller the nanoparticle size which is a common behaviour with metal nanoparticles. There is no specific order observed based on the different concentrations used in this study. Ideally, at higher concentration of the precursor

(AgNO₃), an increase in the formation of nanoparticles is expected as more silver ions would be reduced; but in this work GAgNPs from 1 mM (1:5) showed maximum intensity which reflects larger number of particles. The nature of the surface plasmon bands (SPBs) displayed by the samples from 1 mM concentration using 1:5 volume ratio shows wide spectra range and likely reveals high level of polydispersity with varying sizes of nanoparticles [49].

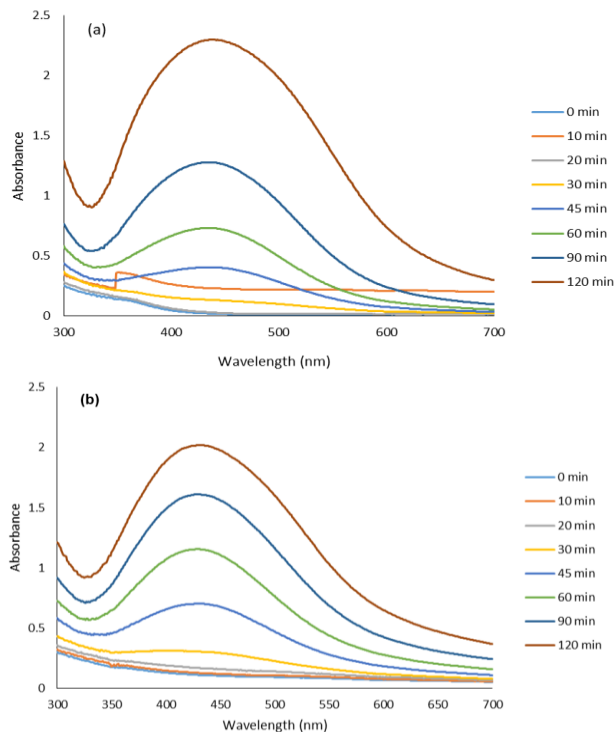


Fig. 2. UV-visible spectra of the nanoparticles synthesized using 2 mM AgNO₃ at (a) 1:5 and (b) 1:10 substrate to precursor.

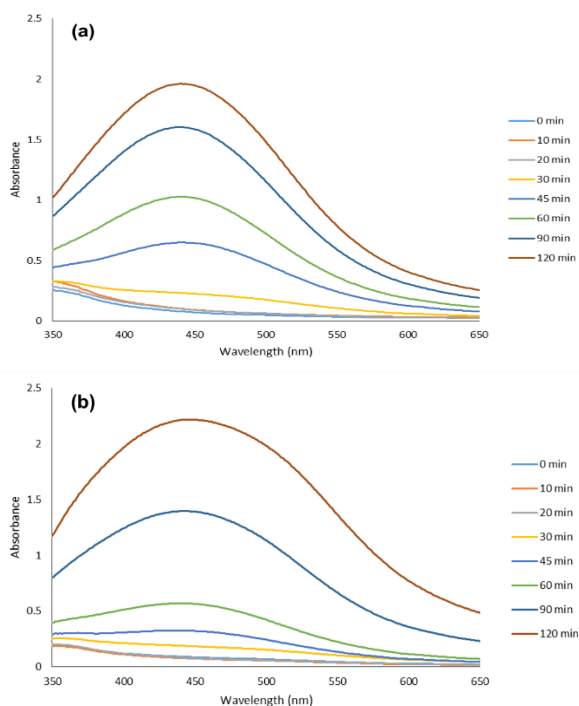


Fig. 3. UV-visible spectra of the nanoparticles synthesized using 5 mM AgNO₃ at (a) 1:5 and (b) 1:10 substrate to precursor.

In the work of Amin *et al.* [50], in which silver nanoparticles were formed by using *solanum xanthocarpum* berry extract, it was observed that as the concentration of the extract increased, the SPBs became sharper and the number of nanoparticles also increased. They also observed that there was a limit to which the biomolecules ceased to act as capping agent and, in that case, an increase in bandwidth occurred which led to anisotropic or larger size particles.

FTIR Spectroscopic analysis of the GAgNPs

FTIR measurement of the plant and the silver nanoparticles obtained using the plant extract was carried out to identify the biomolecules that serve as reducing, capping and stabilizing agents in the synthesized silver nanoparticles. The spectrum of the plant extract (**Fig. 4a**) showed peaks at 3271, 2918, 2854, 2206, 2089, 1726, 1614, 1540, 1417, 1240, 1018 and 522 cm⁻¹. The broad peak in the higher energy region (3272 cm⁻¹) indicates the presence of the OH group in the extract of *Cyamopsis tertagonoloba* [51], while the sharp peaks at 2854 cm⁻¹ and 2919 cm⁻¹ could be due to the stretching vibration of C-H of the alkanes [52]. The weak peaks around 2206, 1462, 1571 cm⁻¹ could be ascribed to the unsaturated aromatic C=C bonds [53], while peaks around 1726 cm⁻¹ corresponds to C=O of esters, ketone or acids. The 1018 cm⁻¹ peak may be due to the stretching vibration of C-H from alkyl halides [54] and the peaks in the range 522 - 507 cm⁻¹ indicates C-Cl stretching of halide groups [55]. In the spectrum of GAgNPs (**Fig. 4b**), the peak positions are similar to that of the plant, but of lower intensity, which indicates capping of the synthesized nanoparticles by the plant extracts. All the absorption bands are summarised in **Table 1**.

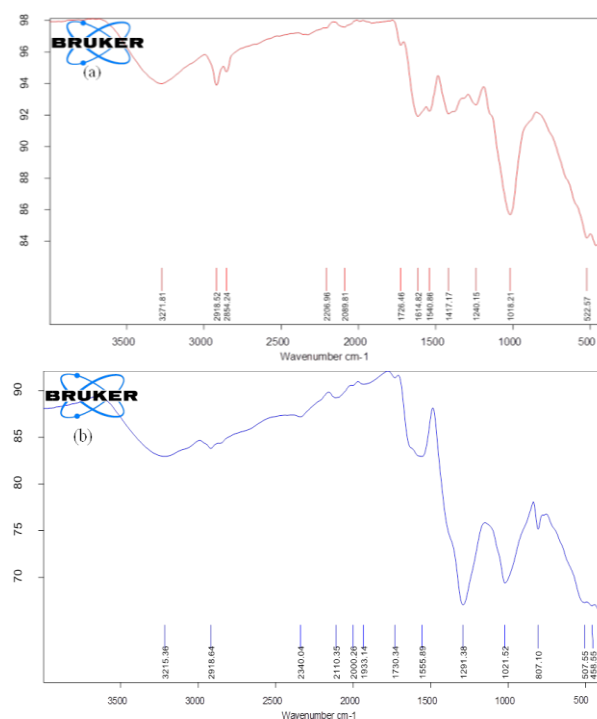


Fig. 4. FTIR spectrum of the (a) Guar Plant and (b) GAgNPs.

Table 1. Functional groups present in the guar plant and nanoparticles.

Functional group	Frequency (cm ⁻¹)		Intensity
	Guar plant	GAgNPs	
OH	3272	3215	Strong, broad
Alkane -C-H	2854, 2919		strong
-C≡C-	2206	2110	Variable
C=C	1571	1540	Medium-weak multiple bands
C=C	1462	1417	Strong
C=O	1739	1726	Strong
C-O	1018		Two bands or more
C-Cl	522	507	Strong

TEM Analysis of the GAgNPs

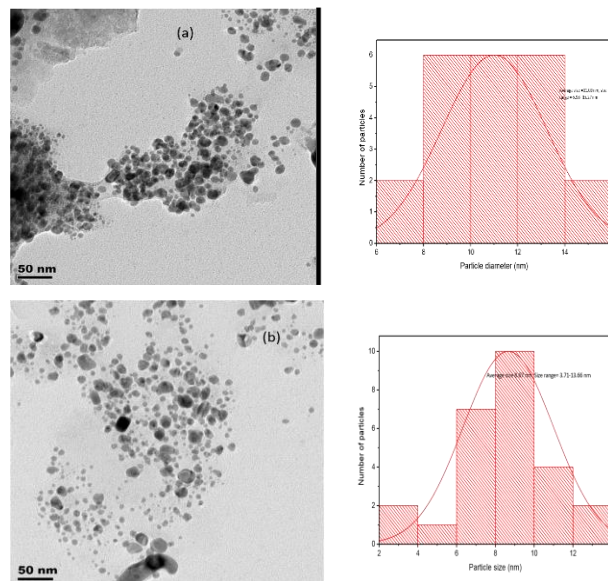
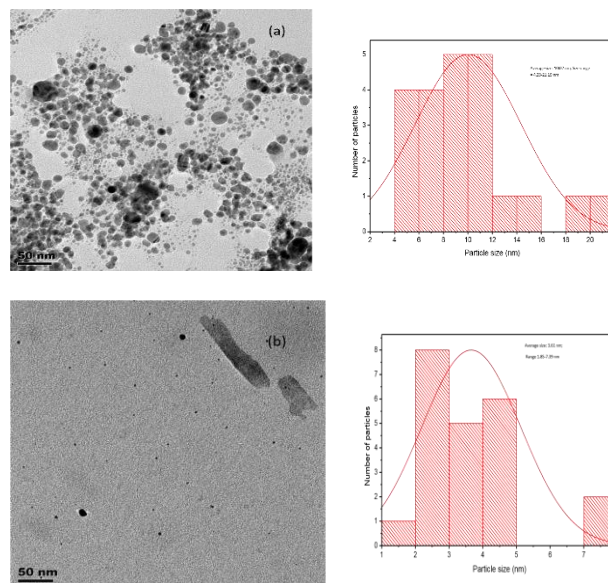
There were variations in the TEM micrographs of the three different concentrations of the precursor used for nanoparticle synthesis as shown in **Figs. 5-7** and **Table 2**. However, in all, nearly spherical shape nanoparticles were obtained. The samples from 2 mM using 1:10 ratio gave the least nanoparticles size, whereas the samples from 5 mM using 1:10 gave the largest size. The lower size ranges of nanoparticles which are monodispersed were mostly recorded with both 1:10 volume ratio of samples obtained from the 1 mM and 2 mM AgNO₃. However, there was a striking appearance of agglomeration in the particles obtained from 2 mM when 1:10 ratio was used. The images obtained in all the concentrations corroborate the results of the UV-vis spectra which showed broad peaks, an indication of polydispersity, except for the particles from 2 mM AgNO₃ using 1:10 volume ratio. The clustered peaks shown by the SPBs of the samples from 1 mM (1:5) illustrate colour changes that lead to varying particle sizes of the nanoparticles which were also confirmed by the TEM image [56]. The samples obtained from 1 mM using 1:5 ratio have the highest number of lower sized nanoparticles which was also shown by the wavelength of absorption compared to other concentrations. However, on the average, the samples from 2 mM (1:10) were recorded to have lowest size of nanoparticles. The mechanism was such that the rate of nuclei formation was higher than the nanoparticle growth rate, thereby giving rise to a large number of smaller particles [57]. In the growth system observed in the particles from 1 mM (1:5), oriented attachment seem to occur as against secondary growth due to Ostwald ripening observed in the particles from 5 mM using 1:10 plant extract to precursor ratio.

The samples obtained from 5 mM using 1:10 ratio have the largest particle size compared to other concentrations used. Different plants behave differently and it could be observed that, in this synthesis, the large size could be due to the low concentration of the substrate (1:10) and the high concentration of the precursor (5 mM). This is comparable to the work of Shukla *et al.* [58], in which the size of the nanoparticles increased with increase in the concentration of the silver nitrate. The amount of active biocomponents that

transform the precursor to their nanoparticles, determines the formation rate of the Ag/AgCl nuclei, the collision rate and general reaction mechanism.

Table 2. Size distribution at different precursor and substrate concentrations of the synthesized GAgNPs.

Concentration of Precursor (AgNO ₃) (mM)	Ratio of Substrate to precursor	Average size of AgNPs (nm)	Size Range (nm)
1	1:5	5.21	2.03-9.36
	1:10	8.67	3.71-13.66
2	1:5	11.00	6.98-15.27
	1:10	3.61	1.85-7.39
5	1:5	10.02	4.23-21.19
	1:10	12.92	6.83-23.43

**Fig. 5.** TEM image and the respective particle size distribution histogram of the nanoparticles obtained from 1 mM AgNO₃ using (a) 1:5 and (b) 1:10 volume ratio of aqueous plant extract: AgNO₃.**Fig. 6.** TEM image and the respective particle size distribution histogram of the nanoparticles obtained from 2 mM AgNO₃ using (a) 1:5 and (b) 1:10 volume ratio of aqueous plant extract: AgNO₃.

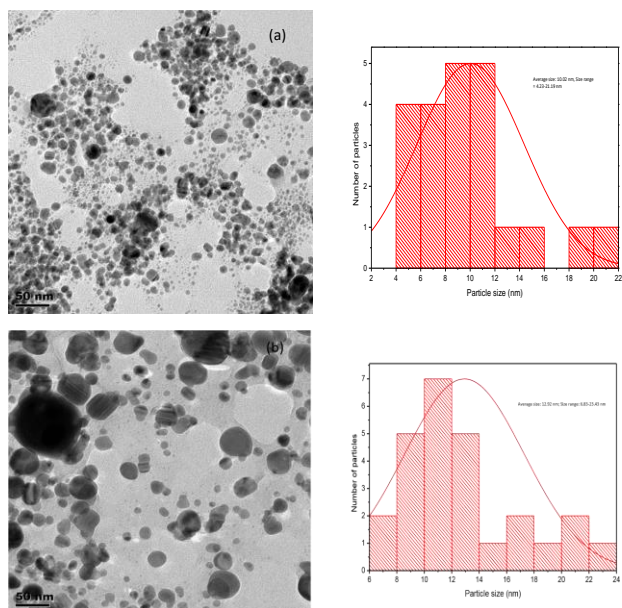


Fig. 7. TEM image and the respective particle size distribution histogram of the nanoparticles obtained from 5 mM AgNO_3 using (a) 1:5 and (b) 1:10 volume ratio of aqueous plant extract: AgNO_3 .

Measurement of zeta potential

Due to the small size and high surface reactivity, attraction or repulsion of the nanoparticles during reaction could occur, thus leading to either agglomeration or dispersion. Zeta potential explains this phenomenon, describes the stability and the surface potential of the nanoparticles [59]. The particles are adjudged stable when their zeta values are more positive than +30 mV or more negative than -30 mV [60]. In the three synthesized nanoparticles with different precursor concentrations, 1 mM, 2 mM and 5 mM, the zeta potential values are -13.6, -14.2 and -15.4 mV respectively as shown in Figs. 8(a-c). These values reflect less stability of the nanoparticles and possibility of agglomeration which is a reflection of the inability of the surface charges to hinder the particles from coalescing. The negativity of the values showed the nanoparticles were capped by the plant biomolecules and also stabilized, although not very efficiently [61]. From the recorded values, stability of the nanoparticles seems to be increasing with higher concentration of the precursor. More so, the type of capping agent or ligand groups used in the nanoparticle synthesis also affects the values of the zeta potential. The knowledge of the degree of stability of nanoparticles aids in their application, thus, very stable nanoparticles would be very useful in pharmaceuticals formulation.

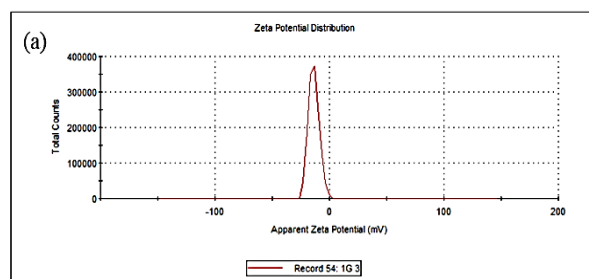
Photocatalytic behaviour of the GAgNPs

The photocatalytic process was monitored at specific time intervals, and the decrease in intensity of absorption at 438 nm was recorded. The percentage degradation was calculated using the equation,

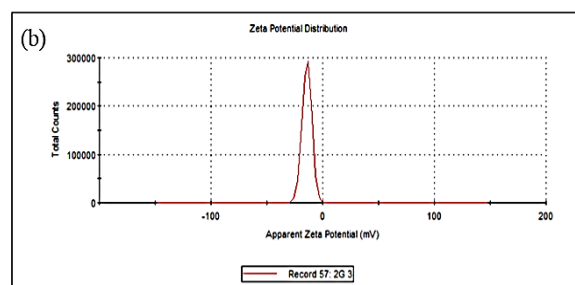
$$\% \text{ Dye degradation} = \frac{C_0 - C_t}{C_0} \times 100 \quad (1)$$

where, C_0 and C_t are the concentration of the dye at initial and specific time t , respectively. Since absorbance is proportional to concentration, the value of the concentrations of the methyl red at the different times were derived from the absorbance peak value at 438 nm. Methyl red ($\text{C}_{15}\text{H}_{15}\text{N}_3\text{O}_2$) is an azo dye, thus carcinogenic and harmful to living organisms [62]. Within the aquatic system, they pose great danger to all living organisms. The mechanism of the photocatalytic reaction could be explained thus:

	Mean (mV)	Area (%)	St Dev (mV)
Zeta Potential (mV): -13.6	Peak 1: -13.6	100.0	4.67
Zeta Deviation (mV): 4.67	Peak 2: 0.00	0.0	0.00
Conductivity (mS/cm): 0.210	Peak 3: 0.00	0.0	0.00
Result quality : Good			



	Mean (mV)	Area (%)	St Dev (mV)
Zeta Potential (mV): -14.2	Peak 1: -14.2	100.0	4.33
Zeta Deviation (mV): 4.33	Peak 2: 0.00	0.0	0.00
Conductivity (mS/cm): 0.137	Peak 3: 0.00	0.0	0.00
Result quality : Good			



	Mean (mV)	Area (%)	St Dev (mV)
Zeta Potential (mV): -15.4	Peak 1: -15.4	100.0	4.09
Zeta Deviation (mV): 4.09	Peak 2: 0.00	0.0	0.00
Conductivity (mS/cm): 0.187	Peak 3: 0.00	0.0	0.00
Result quality : Good			

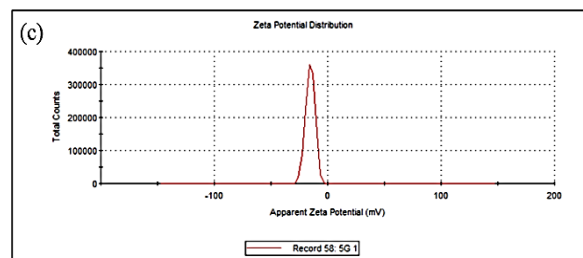


Fig. 8. Surface zeta potential graph of GAgNPs synthesized using (a) 1 mM, (b) 3 mM and (c) 5 mM precursor concentration.

The nanoparticles absorb ultraviolet radiation, causing the surface to be activated and electrons are excited; these photogenerated electrons interact with the dissolved oxygen molecules to yield O_2^- radicals that can degrade the organic dye [63].

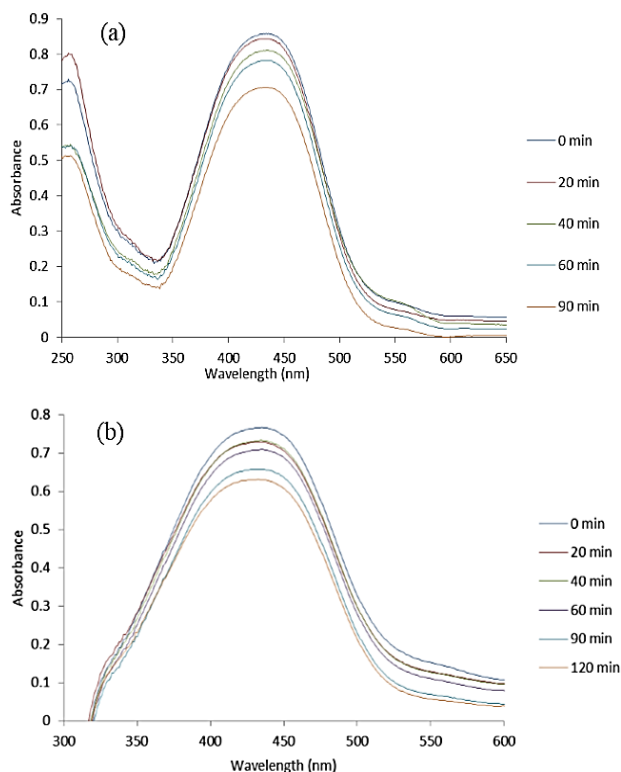


Fig. 9. Degradation of methyl red using GAgNPs obtained from (a) 1 mM and (b) 5mM AgNO₃ using 1:5 volume ratio of AgNO₃ to aqueous leaf extract.

At 438 nm, the % degradation recorded for the samples obtained from 1 mM AgNPs was 17%, while for the 5 mM samples, it was 14% after 90 min reaction as shown in **Figs. 9 a** and **b**, and presented in **Table 3**. The values show low percentage degradation compared to other literature reports. Perhaps, there was no effective activation of the surfaces of the silver nanoparticles and therefore, intermediate molecules such as the dissolved oxygen radicals which could lead to efficient degradation were not sufficiently produced. The results recorded here reiterate the fact that photocatalytic behaviour of nanoparticles is prominently due to their band structure [64].

Table 3. Percentage photocatalytic degradation recorded at 438 nm at different time intervals

Time (min)	1 mm (1:5)		5 mm (1:5)	
	Absorbance	% degradation	Absorbance	% degradation
0	0.8556	-	0.7651	
20	0.8421	1.58	0.7307	4.50
40	0.8088	5.47	0.7305	4.52
60	0.7804	8.79	0.7076	7.52
90	0.7049	17.61	0.6562	14.40
120	0.7050	17.62	0.6285	17.85

Antibacterial analysis

The antibacterial studies of the nanoparticles was carried out using some selected bacteria that pose lot of challenges to health and the results are presented in **Table 4**. Silver has great antibacterial properties, likewise some plant extracts. It is, therefore, believed that the synergistic antibacterial property would arise from the combination of the silver, the plant extract in the nanoparticles, in addition to the positive effect of the small sizes. The mechanism of the activity is such that there is penetration of the small nanoparticles into the disease causing microorganisms, thereby binding with the cell membrane and quenching their activities. During the analysis, there was no inhibition seen below 20 µg/mL nanoparticle solution but at concentration of about 25 µg/mL, the growth of the micro-organisms was inhibited. The bacterial strains then become vulnerable and the nanoparticles became active.

E. coli and *K. pneumonia* which are gram negative organisms gave the highest zone of inhibition compared to *Staphylococcus aureus* and *Bacillus cereus* which are gram positive bacteria (**Table 4**). The reason is attributed to the cell wall of the gram positive bacteria being more robust and therefore tends to be resistant to attacks [65, 66]. The antibacterial activity of the silver nanoparticles in this research may be considered to be effective when compared with some literature reports [67]. The extracts from Guar leaf have been reported to be active against bacteria organisms [68], but the AgNPs have higher activity due to the surface characteristics of the nanoparticles which enables the isolates to be absorbed on the surfaces.

Table 4. Antibacterial results of AgNPs (Zone of inhibition in mm).

Samples	<i>Staphylococcus aureus</i>	<i>Bacillus cerues</i>	<i>Klebsiella. pneumonia</i>	<i>Escherichia. Coli</i>
GAgNPs	10.5 ± 0.0	8.2 ± 0.7	11.2 ± 0.3	14.7 ± 1.2
Ciprofloxacin	20.0 ± 1.4	25.8 ± 0.0	23.0 ± 0.0	25.0 ± 0.7
Water	R	R	R	R

Values (in mm) represent the mean of double replications and their standard deviation; standard drug (Ciprofloxacin) was used as positive control for antibacterial studies, water was used as negative control and showed no activity, R = resistant. The well diameter was 6 mm, and any activity below 6 mm was considered resistant.

Table 5 shows the minimum inhibitory concentrations (MIC) of the samples, and it shows that the MIC against *S. aureus* and *E.coli* are lower than 0.05 mg/mL which was the same concentration as the control drug, ciprofloxacin. In general, the nanoparticles showed some great potency towards inhibition of bacterial growth especially *E.coli* but the control drug was more active.

Table 5. Minimum inhibitory concentration (MIC).

Samples	<i>Staphylococcus aureus</i>	<i>Bacillus cerues</i>	<i>Kleb. pneumonia</i>	<i>E. Coli</i>
AgNPs	<0.05	0.1	0.1	<0.05
Ciprofloxacin	<0.05	<0.05	<0.05	<0.05

Conclusion

The extensive research on plant mediated synthesis of noble metal nanoparticles is due to the different degrees of the constituent plant biomolecules and the ability of the synthesized nanoparticles to offer various applications. In this investigation, the synthesis of silver nanoparticles using guar plant as substrate increased the already existing information on various silver nanoparticles made by different plants. In addition, reaction conditions were varied in order to explore the behaviour of the nanoparticles and how their properties are affected. Three different precursor concentrations (1 mM, 2 mM, 5 mM) were used in the synthesis and two volume ratios (1:5, 1:10) of plant extract to the precursor. The obtained results indicated that the 5 mM precursor concentration gave rise to larger particle sizes, while the 1 mM concentration has the smallest particle sizes. Slight agglomeration of particles occurred which suggested some attraction, resulting in low stability, with the nanoparticles obtained from 5 mM of the precursor being the most stable. The photocatalytic behaviour against methyl red is low based on the duration of time studied but are promising. Nanoparticles may act differently as photocatalysts depending on the pollutants or dyes and also on the time of reaction. The nanoparticles showed some antibacterial activity, against four different bacteria strains with *E. coli* being the most vulnerable.

References

- Khan, I.; Saeed, K.; Khan, I., Nanoparticles: Properties, applications and toxicities, *Arab. J. Chem.*, **2017**.
DOI: 10.1016/j.arabjc.2017.05.011
- Khodashenas, B.; Ghorbani, H. R., Synthesis of silver nanoparticles with different shapes, *Arab. J. Chem.*, **2015**.
DOI: 10.1016/j.arabjc.2014.12.014
- Nair, L.S.; Laurencin, C.T., Silver nanoparticles: Synthesis and therapeutic applications, *J. Biomed. Nanotechnol.*, **2007**, 3, 301.
DOI: 10.1166/jbn.2007.041
- Lee, K.S.; El-Sayed, M.A., Gold and silver nanoparticles in sensing and imaging: Sensitivity of plasmon response to size, shape, and metal composition, *J. Phys. Chem. B*, **2006**, 110, 19220.
DOI: 10.1021/jp062536y
- Wijnhoven, S.W.P.; Peijnenburg, W.J.G.M.; Herberts, C.A.; Hagens, W.I.; Oomen, A.G.; Heugens, E.H.W., Nano-silver: A review of available data and knowledge gaps in human and environmental risk assessment, *Nanotoxicology*, **2009**, 3, 109.
DOI: 10.1080/17435390902725914
- Ahmed, S.; Saifullah, Ahmad, M.; Swami, B. L.; Ikram, S., Green synthesis of silver nanoparticles using *azadirachta indica* aqueous leaf extract, *J. Rad Res. Appl. Sci.* **2016**, 9, 1.
DOI: 10.1016/j.jrras.2015.06.006
- Yilmaz, M.; Turkdemir, H.; Kilic, M.A.; Bayram, E.; Cicek, A.; Mete, A.; Ulug, B., Biosynthesis of silver nanoparticles using leaves of *Stevia Rebaudiana*, *Mater. Chem. Phys.*, **2011**, 130, 1195.
DOI: 10.1016/j.matchemphys.2011.08.068
- Gurunathan, S.; Han, J.W.; Kwon, D.N.; Kim, J.H., Enhanced antibacterial and anti-biofilm activities of silver nanoparticles against Gram-negative and Gram-positive bacteria, *Nanoscale Res. Lett.*, **2014**, 9, 373.
DOI: 10.1186/1556-276X-9-373
- Ghorbani, H.R.; Attar, H.; Safekordi, A.A.; Sorkhabadi, S.M., Design of a bioprocess to produce silver nanoparticles, *IET Nanobiotechnol*, **2012**, 6, 71.
DOI: 10.1049/iet-nbt.2011.0035
- Rasheeda, T.; Bilal, M.; Iqbal, H.M.N.; Li C., Green biosynthesis of silver nanoparticles using leaves extract of *Artemisia vulgaris* and their potential biomedical applications, *Col. Surf. B: Biointerfaces*, **2017**, 158, 408.
DOI: 10.1016/j.colsurfb.2017.07.020
- Zhang, X.F.; Liu, Z.G.; Shen, W.; Gurunathan, S., Silver Nanoparticles: Synthesis, Characterization, Properties, Applications, and Therapeutic Approaches, *Int. J. Mol. Sci.*, **2016**, 17, 1534.
DOI: 10.3390/ijms17091534
- Noruzi, M., Biosynthesis of gold nanoparticles using plant extracts, *Bioprocess Biosyst. Eng.* **2015**, 38, 1.
DOI: 10.1007/s00449-014-1251-0
- Elemike, E. E.; Oge, M. A.; Onwudiwe, D. C.; Ayeni, M. B.; Mgbemena, C. O., Kinetics of fresh and fermented palm wine (*Raphia hookeri*) biosynthesized silver nanoparticles and their antibacterial activities, *J. Chin. Adv. Mat. Soc.*, **2017**, 6, 17.
DOI: 10.1080/22243682.2017.1383183
- Sur, U. K.; Ankamwar, B.; Karmakar, S.; Halder, A.; Das, P., Green synthesis of Silver nanoparticles using the plant extract of *Shikakai* and *Reetha*, *Materials Today: Proc.*, **2018**, 5, 2321.
DOI: 10.1016/j.matpr.2017.09.236
- Upadhyay, L. S. B.; Verma, N., Recent Developments and Applications in Plant-extract Mediated Synthesis of Silver Nanoparticles, *Anal. Letts.*, **2015**, 48, 2676.
DOI: 10.1080/00032719.2015.1048350
- Roy, P.; Das, B.; Mohanty, A.; Mohapatra, S., Green synthesis of silver nanoparticles using *Azadirachta indica* leaf extract and its antimicrobial study, *Appl. Nanosci.*, **7**, **2017**, 843.
DOI: 10.1007/s13204-017-0621-8
- Banerjee, P.; Satapathy, M.; Mukhopahayay, A.; Das, P., Leaf extract mediated green synthesis of silver nanoparticles from widely available Indian plants: synthesis, characterization, antimicrobial property and toxicity analysis, *Bioresour. Bioprocess*, **2014**, 1, 1.
DOI: 10.1186/s40643-014-0003-y
- Pal, S.; Tak, Y.K.; Song, J.M., Does the antibacterial activity of silver nanoparticles depend on the shape of the nanoparticle? A study of the gram-negative bacterium *Escherichia coli*, *Appl. Environ. Microbiol.*, **2007**, 73, 1712.
DOI: 10.1128/AEM.02218-06
- Gurunathan, S.; Jeong, J.K.; Han, J.W.; Zhang, X.F.; Park, J.H.; Kim, J.H., Multidimensional effects of biologically synthesized silver nanoparticles in *Helicobacter pylori*, *Helicobacter felis*, and human lung (L132) and lung carcinoma A549 cells, *Nanoscale Res. Lett.*, **2015**, 10, 1.
DOI: 10.1186/s11671-015-0747-0
- Veerasingam, R.; Xin, T. Z.; Gunasagar, S.; Xiang, T. F. W.; Yang, E. F. C.; Jayakumar, N.; Dhanaraj, S. A., Biosynthesis of silver nanoparticles using mangosteen leaf extract and evaluation of their antimicrobial activities, *J. Saudi Chem. Soc.*, **2011**, 15, 113.
DOI: 10.1016/j.jscs.2010.06.004
- Ge, L.; Li, Q.; Wang, M.; Ouyang, J.; Li, X.; Xing, M. M., Nanosilver particles in medical applications: synthesis, performance, and toxicity, *Int. J. Nanomed.*, **2014**, 9, 2399.
DOI: 10.2147/IJN.S55015
- Loo, C.; Lowery, A.; Halas, N.; West, J.; Drezek, R., Immunotargeted nanoshells for integrated cancer imaging and therapy, *Nano Lett.*, **2005**, 5, 709.
DOI: 10.1021/nl050127s
- Zhou, W.; Ma, Y.Y.; Yang, H.; Ding, Y.; Luo, X.G., A label-free biosensor based on silver nanoparticles array for clinical detection of serum p53 in head and neck squamous cell carcinoma, *Int. J. Nanomed.*, **2011**, 6, 381.
DOI: 10.2147/IJN.S13249
- Jun, B.H.; Noh, M.S.; Kim, J.; Kim, G.; Kang, H.; Kim, M.S.; Seo, Y.T.; Baek, J.; Kim, J.H.; Park, J.; Kim, S.; Kim, Y.K.; Hyeon, T.; Cho, M.H.; Jeong, D.H.; Lee, Y.S., Multifunctional silver-embedded magnetic nanoparticles as SERS nanoprobes and their applications, *Small*, **2010**, 6, 119.
DOI: 10.1002/smll.200901459
- Pattanayak, S.; Mollick, M. M. R.; Maity, D.; Chakraborty, S.; Dash, S. K.; Chattopadhyay, S.; Roy, S.; Chattopadhyay, D.; Chakraborty, M., *Butea monosperma* bark extract mediated

- green synthesis of silver nanoparticles: Characterization and biomedical applications. *J. Saudi Chem. Soc.*, **2017**, *21*, 673.
DOI: 10.1016/j.jscs.2015.11.004
26. Sondi, I.; Salopek-Sondi, B., Silver nanoparticles as antimicrobial agent: A case study on *E. coli* as a model for Gram-negative bacteria. *J. Colloid Interf. Sci.*, **2004**, *275*, 177.
DOI: 10.1016/j.jcis.2004.02.012
27. Padalia, H.; Moteriy, P.; Chanda, S., Green synthesis of silver nanoparticles from marigold flower and its synergistic antimicrobial potential. *Arab. J. Chem.*, **2015**, *8*, 732.
DOI: 10.1016/j.arabjc.2014.11.015
28. Elumalai, E.K.; Prasad, T.N.V.K.V.; Hemachandran, J.; Therasa, S.V.; Thirumalai, T.; David, E., Extracellular synthesis of silver nanoparticles using leaves of *Euphorbia hirta* and their antibacterial activities. *J. Pharm. Sci. Res.*, **2010**, *2*, 549.
DOI: 10.1.1.175/j.jpsr.2010.434
29. Naghdi, M.; Taheran, M.; Brar, S.K.; Verma, M.; Surampalli, R.Y.; Valero, J.R., Green and energy-efficient methods for the production of metallic nanoparticles Beilstein *J. Nanotechnol.*, **2015**, *6*, 2354.
DOI: 10.3762/bjnano.6.243
30. Elemike, E.E.; Onwudiwe, D.C.; Ekennia, A.C.; Sonde, C.U.; Ehiri, R.C., Green Synthesis of Ag/Ag₂O Nanoparticles Using Aqueous Leaf Extract of *Eupatorium odoratum* and Its Antimicrobial and Mosquito Larvicidal Activities. *Molecules*, **2017**, *22*, 674.
DOI: 10.3390/molecules22050674
31. Etheridge, M.L.; Campbell, S.A.; Erdman, A.G.; Haynes, C.L.; Wolf, S.M.; McCullough, J., The big picture on small medicine: The state of nanomedicine products approved for use or in clinical trials. *Nanomed.*, **2013**, *9*, 1.
DOI: 10.1016/j.nano.2012.05.013
32. Mallick, K.; Witcomb, M.; Scurrell, M., Silver nanoparticle catalysed redox reaction: An electron relay effect. *Mater. Chem. Phys.*, **2006**, *97*, 283.
DOI: 10.1016/j.matchemphys.2005.08.011
33. Elemike, E. E.; Onwudiwe, D. C.; Mkhize, Z., Ecofriendly synthesis of AgNPs using *Verbascum thapsus* extract and its photocatalytic activity. *Mat. Lett.*, **2016**, *185*, 452.
DOI: 10.1016/j.matlet.2016.09.026
34. Gadkari, R. R.; Ali, S. W.; Alagirusamy, R.; Das, A., Silver Nanoparticles in Water Purification: Opportunities and Challenges. **2017**, 229.
DOI: 10.1007/978-3-319-64501-8_13
35. Chahardoli, A.; Karimi, N.; Fattahi, A., *Nigella arvensis* leaf extract mediated green synthesis of silver nanoparticles: Their characteristic properties and biological efficacy. *Adv. Powder Technol.*, **2018**, *29*, 202.
DOI: 10.1016/j.apt.2017.11.003
36. Ajitha, B.; Reddy, Y. A. K.; Jeon, H. J.; Ahn, C.W., Synthesis of silver nanoparticles in an eco-friendly way using *Phyllanthus amarus* leaf extract: Antimicrobial and catalytic activity. *Adv. Powder Technol.*, **2018**, *29*, 86.
DOI: 10.1016/j.apt.2017.10.015
37. Ibrahim, H.M.M., Green synthesis and characterization of silver nanoparticles using banana peel extract and their antimicrobial activity against representative microorganisms. *J. Rad. Res. Appl. Sci.*, **2015**, *8*, 265.
DOI: 10.1016/j.jrras.2015.01.007
38. Singhal, G.; Bhavesh, R.; Kasariya, K.; Sharma, A. R.; Singh, R. P., Biosynthesis of silver nanoparticles using *Ocimum sanctum* (Tulsi) leaf extract and screening its antimicrobial activity. *J. Nanopart. Res.*, **2011**, *13*, 2981.
DOI: 10.1007/s11051-010-0193-y
39. Kim, D Y.; Saratale, R. G.; Shinde, S.; Syed, A.; Ameen, F.; Ghodake, G., Green synthesis of silver nanoparticles using *Laminaria japonica* extract: Characterization and seedling growth assessment. *J. Cleaner Prod.*, **2018**, *172*, 2910.
DOI: 10.1016/j.jclepro.2017.11.123
40. Kumar, B.; Smita, K.; Cumbal, L.; Debut, A., Green synthesis of silver nanoparticles using Andean blackberry fruit extract. *Saudi J. Biol. Sci.*, **2017**, *24*, 45.
DOI: 10.1016/j.sjbs.2015.09.006
41. Pathak, R.; Singh, S. K.; Singh, M.; Henry, A., Molecular assessment of genetic diversity in cluster bean (*Cyamopsis tetragonoloba*) genotypes. *J. Genetics.*, **2010**, *89*, 243.
DOI: 10.1007/s12041-010-0033-y
42. Mudgil, D.; Barak, S.; Khatkar, B. S., Guar gum: Processing, properties and food applications - A Review. *J. Food Sci. Tech.*, **2014**, *51*, 409.
DOI: 10.1007/s13197-011-0522-x
43. Raghavendra, C.K.; Srinivasan, K., Potentiation of anti-cholelethogenic influence of dietary tender cluster beans (*Cyamopsis tetragonoloba*) by garlic (*Allium sativum*) in experimental mice. *Indian J. Med Res.*, **2015**, *142*, 462.
DOI: 10.4103/0971-5916.169214
44. Gresta, F.; Ceravolo, G.; Presti, V. L.; Agata, A.; Rao, R.; Chiofalo, B., Seed yield, galactomannan content and quality traits of different guar (*Cyamopsis tetragonoloba* L.) genotypes. *Ind. Crop Prod.*, **2017**, *107*, 122.
DOI: 10.1016/j.indcrop.2017.05.037
45. Butt, M. S.; Shahzadi, N.; Sharif, M. K.; Nasir, M., Guar Gum: A Miracle Therapy for Hypercholesterolemia, Hyperglycemia and Obesity. *Crit. Rev. Food Sci. Nutr.* **2007**, *47*, 389.
DOI: 10.1080/10408390600846267
46. Elemike, E.E.; Fayemi, O.E.; Ekennia, A.C.; Onwudiwe, D.C.; Ebenso, E.E., Silver Nanoparticles Mediated by *Costus afer* Leaf Extract: Synthesis, Antibacterial, Antioxidant and Electrochemical Properties. *Molecules*, **2017**, *22*, 701.
DOI: 10.3390/molecules22050701
47. Ali, Z. A.; Yahya, R.; Sekaran, S. D.; Put, R., Green Synthesis of Silver Nanoparticles Using Apple Extract and Its Antibacterial Properties. *Adv. Mat. Sci. Eng.*, **2016**, *1*.
DOI: 10.1155/2016/4102196
48. Gharibshahi, E.; Saion, E., Influence of Dose on Particle Size and Optical Properties of Colloidal Platinum Nanoparticles. *Int. J. Mol. Sci.*, **2012**, *13*, 14723.
DOI: 10.3390/ijms131114723
49. Liz-Marzan, L. M., Tailoring Surface Plasmons through the Morphology and Assembly of Metal Nanoparticles. *Langmuir*, **2006**, *22*, 32.
DOI: 10.1021/la0513353
50. Amin, M.; Anwar, F.; Janjua, M. R. S. A.; Iqbal, M. A.; Rashid, U., *Int. J. Mol. Sci.*, **2012**, *13*, 9923.
DOI: 10.3390/ijms13089923
51. Ahmed, S.; Ikraam, S., Silver Nanoparticles: One Pot Green Synthesis Using *Terminalia arjuna* Extract for Biological Application. *J. Nanomed Nanotechnol.*, **2015**, *6*, 309.
DOI: 10.4172/2157-7439.1000309
52. Sadeghi, B.; Gholamhoseinpoor, F., A Study on Stability and Green Synthesis of Silver Nanoparticles Using *Ziziphora tenuior* (Zt) Extract at Room Temperature. *Spectrochim. Acta A.*, **2015**, *134*, 310.
DOI: 10.1016/j.saa.2014.06.046
53. Prabu, H.J.; Johnson, I., Plant-mediated biosynthesis and characterization of silver nanoparticles by leaf extracts of *Tragia involucrata*, *Cymbopogon citronella*, *Solanum verbascifolium* and *Tylophora ovata*. *Karbala Int. J. Modern Sci.*, **2015**, *1*, 237.
DOI: 10.1016/j.kijoms.2015.12.003
54. Premasudha P.; Venkataramana M.; Abirami M.; Vanathi P.; Karishna K.; Rajendran R., Biological synthesis and characterization of silver nanoparticles using *Eclipta alba* leaf extract and evaluation of its cytotoxic and antimicrobial potential. *Bull. Mater. Sci.*, **2015**, *38*, 965.
DOI: 10.1007/s12034-015-0945-5
55. Jyoti, K.; Baunthiyal, M.; Singh, A., Characterization of silver nanoparticles synthesized using *Urtica dioica* Linn. leaves and their synergistic effects with antibiotics. *J. Radiat. Res. Appl. Sci.*, **2016**, *9*, 217.
DOI: 10.1016/j.jrras.2015.10.002
56. Vanaja, M.; Annadurai G., *Coleus aromaticus* leaf extract mediated synthesis of silver nanoparticles and its bactericidal activity. *Appl. Nanosci.*, **2013**, *3*, 217.
DOI: 10.1007/s13204-012-0121-9
57. Kato, H.; Nakamura, A.; Takahashi, K.; Kinugasa, S., Size effect on UV-Vis absorption properties of colloidal C60 particles in water. *Phys. Chem.*, **2009**, *11*, 4946.
DOI: 10.1039/B904593G
58. Shukla, P.; Nandi, T.; Singh, R. P., Synthesis of Sorbitan Ester Stabilized Uniform Spherical Silver Nanoparticles. *Orient. J. Chem.*, **2016**, *32*, 2947.
DOI: 10.13005/ojc/320614

59. Srikar, S.K.; Giri, D.D.; Pal, D.B.; Mishra, P.K.; Upadhyay, S.N. Green Synthesis of Silver Nanoparticles: A Review, *Green and Sustainable Chem.*, **2016**, *6*, 34.
DOI: 10.4236/gsc.2016.61004
60. Saeb, A. T. M.; Alshammari, A. S.; Al-Brahim, H.; Al-Rubeaan, K. A., Production of Silver Nanoparticles with Strong and Stable Antimicrobial Activity against Highly Pathogenic and Multidrug Resistant Bacteria, *Sci. World J.*, **2014**, *2014*, 1.
DOI: 10.1155/2014/704708
61. Meléndrez, M. F.; Cárdenas, G.; Arbiol, J., Synthesis and characterization of gallium colloidal nanoparticles, *J. Col. Interf. Sci.*, **2010**, *346*, 279.
DOI: 10.1016/j.jcis.2009.11.069
62. Selvam, G. G.; Sivakumar. K., Phycosynthesis of silver nanoparticles and photocatalytic degradation of methyl orange dye using silver (Ag) nanoparticles synthesized from *Hypnea musciformis* (Wulfen) J.V. Lamouroux, *J. Appl. Nano Sci.*, **2014**, *5*, 617.
DOI: 10.1007/s13204-014-0356-8
63. Park, H.; Kim, H.; Moon, G.; Cho W., Photoinduced charge transfer processes in solar photocatalysis based on modified TiO₂, *Energy Environ. Sci.*, **2016**, *9*, 411.
DOI: 10.1039/C5EE02575C
64. Zhao, X.; Zhang, J.; Wang, B.; Zada, A.; Humayun, M., Biochemical Synthesis of Ag/AgCl Nanoparticles for Visible-Light-Driven Photocatalytic Removal of Colored Dyes, *Materials*, **2015**, *8*, 2043.
DOI: 10.3390/ma8052043
65. Onwudiwe, D.C.; Ekennia, A.C.; Hosten. E., Syntheses, characterization, and antimicrobial properties of nickel (II) dithiocarbamate complexes containing NiS₄ and NiS₂PN moieties, *J. Coord. Chem.*, **2016**, *69*, 2454.
DOI: 10.1080/00958972.2016.1186800
66. Satyavani, K.; Ramanathan, T.; Gurudeeban, S., Low-cost and eco-friendly phyto-synthesis of Silver nanoparticles by using grapes fruit extract and study of antibacterial and catalytic effects, *Dig. J. Nanomater. Biostruct.*, **2011**, *6*, 1019.
DOI: 10.22034/IJND.2017.24376
67. Adur, A. J.; Nandini, N.; Shilpashree, M. K.; Ramya, R.; Srinatha, N., Bio-synthesis and antimicrobial activity of silver nanoparticles using anaerobically digested parthenium slurry, *J. Photochem. Photobiol. B*, **2018**, *183*, 30.
DOI: 10.1016/j.jphotobiol.2018.04.020
68. Gheisari, A.A.; Zavareh, M.S.; Toghyani, M.; Bahadoran, R.; Toghyani, M., Application of incremental program, an effective way to optimize dietary inclusion rate of guar meal in broiler chicks, *Livestock Sci.*, **2011**, *140*, 117
DOI: 10.1016/j.livsci.2011.02.018